El Cezeri
Journal of Science and Engineering
ISSN: 2148-3736

Research Article

# Research of Glass-Ceramic Material Synthesis Through Waste By-Product Sintering from Mining and Metallurgical Activities

**Oktay Bayat[1a], Mahmut Altiner[1b], Muhammed Aboelgamel[1c]**

[1]Mining Engineering Department, Çukurova University, Adana, 01330, Türkiye

obayat@cu.edu.tr

DOI: 10.31202/ecjse.1654765
Received: 10.03.2025 Accepted: 09.12.2025
**How to cite this article:**
Bayat O., Altiner M., and Aboelgamel M, "Research of Glass-Ceramic Material Synthesis Through Waste By-Product Sintering from Mining and Metallurgical Activities", El-Cezeri Journal of Science and Engineering, Vol: 13, Iss: 2, (2026), pp.(125-134).
ORCID: [a]0000-0003-2330-3074, [b]0000-0002-7428-5999, [c]0009-0006-4126-8347.

**Abstract** This study analyzes the possibility of producing glass-ceramics from chromite tailings, coal fly ash (Class F), and red mud industrial wastes in Türkiye. Unlike previous studies that typically used binary mixtures or different compositional ratios, this study introduces a novel ternary combination with a fixed 1:2:3 ratios (fly ash: chromite tailings: red mud)**.** This specific ratio was optimized through experimental trials and found to enhance sinterability, mechanical strength, and microstructural stability. The glass-ceramics obtained using this ratio demonstrated compressive strength, water absorption, and density of 12.21 MPa, 0.44%, and 2.05 g/cm³, respectively. The resultant products were analyzed by XRD and leaching tests, which confirmed quartz-based crystalline phases and negligible leaching of toxic metal ions. These findings propose a new strategy for environmentally benign waste recycling, aligned with green chemistry principles and the UN Sustainable Development Goal 12.

**Keywords:** Sintering, Glass-ceramics, Refractories, Mining tailings

## 1. INTRODUCTION

The production of glass-ceramics from mining and metallurgical wastes as composite materials offers a promising pathway for both waste utilization and recycling. Such materials have potential applications across various industrial sectors, including factory flooring, heat-resistant utensils, and other engineering products. They comply with compositional, toxicity leaching, and processing standards, demonstrating their feasibility as ideal industrial products [1, 2]. The generation of solid wastes and the resulting environmental pollution from mining and metallurgical operations necessitate the development of robust waste management policies. In Türkiye, chromite mining alone produced approximately 6.5 million tons of solid tailings in 2021 [3]. Additionally, the Bayer process used for alumina production from bauxite generates red mud as a by-product—typically amounting to 1–1.5 times the mass of the alumina extracted. The Seydişehir (Konya, Türkiye) alumina refinery produces about 200,000 tons of alumina annually, accompanied by roughly 300,000 tons of solid red mud residues [2] [4]. Moreover, over 50 coal-fired power plants in Türkiye generate more than 13 million tons of fly ash each year (both Class C and Class F). Despite this, the utilization rate of fly ash remains considerably lower than that of developed countries, particularly in applications such as building materials and concrete production [5-7]. In response to this need, numerous national and international studies have been conducted to enhance the economic value of fly ash while simultaneously mitigating its environmental impact.

In this research, solid wastes from chromite mining, red mud, and fly ash were used to produce glass-ceramic building materials through the sintering method, with quartzite, china clay, and sodium carbonate serving as additives. Previous studies [8-27] have explored various industrial waste sources for their potential in glass-ceramic production, primarily focusing on waste utilization and recycling. Most of these earlier works [9, 12, 13, 15, 22, 28] investigated binary mixtures—such as red mud–chromite tailings or fly ash–industrial waste—at different compositional ratios. However, no comprehensive study has yet examined the specific ternary mixture (fly ash: chromite tailings: red mud = 1: 2: 3) employed in this research. The synergistic combination of these three waste materials in this ratio was found to enhance sinterability, mechanical strength, and heavy metal immobilization efficiency. This experimental study provides a valuable technical reference for the simultaneous disposal and valorization of mining and metallurgical wastes through glass-ceramic production.

## 2. MATERIALS

Chromite tailings were obtained from a local chromite mining company (Akmetal, Adana, Türkiye). Red mud was supplied by Eti Alüminyum Corp. Fly ash (Class F, as defined in ASTM C618) was collected from the Sugözü Thermal Power Plant (Türkiye). Kaolin was provided by Zafer Maden (Balıkesir, Türkiye), and quartzite was supplied by a local supplier. Poly(vinyl alcohol) (PVOH, PVA, or PVAl), a water-soluble synthetic polymer with the general formula $[CH_2CH(OH)]_n$, was used as a binding agent for all experiments. It was supplied by Sigma-Aldrich (Product No. 341584; CAS No. 9002-89-5). Sodium carbonate ($Na_2CO_3$) of analytical grade (CAS No. 497-19-8) was also used as an additive and obtained from a local supplier.

## 3. METHODS

Mineralogical analysis of the raw materials was conducted using a PANalytical EMPYREAN powder X-ray diffractometer (Cu Kα radiation, 20–50 kV, 5–60 mA) with a scanning range of 2θ = 5–70° and a step rate of 2°/min. Phase identification was performed using *HighScore Plus* software with the COD 2020 database. Particle size distribution was determined by the dry mechanical sieving method for particles coarser than 75 μm, while a *Malvern Mastersizer 3000* instrument was used for sub-sieve fractions (<75 μm). Elemental (oxide) compositions of the wastes and additives were analyzed using a *PANalytical MiniPal* X-ray fluorescence (XRF) spectrometer following the standard DIN 51001 [29]. For verification, hydrofluoric acid digestion followed by atomic absorption spectrophotometry (AAS) was also applied. Loss on ignition (LOI) was determined by heating pre-weighed dry samples (dried at 105 °C) at 1000 °C for 2 h, followed by cooling in a desiccator. Table 1 presents the chemical compositions and sources of the solid wastes and additives used in glass-ceramic production.

**Table 1: Chemical analysis of the waste samples and additives used in the batch preparation.**

| Oxide, wt. % | Chromite waste (tailings) | Red mud | Fly Ash (Class F) | Quartzite | Kaolin |
|---|---|---|---|---|---|
| $SiO_2$ | 43.00 | 15.46 | 46.00 | 98.47 | 71.67 |
| $Al_2O_3$ | - | 18.87 | 23.00 | 0.40 | 18.25 |
| $Fe_2O_3$ | 37.30 | 35.56 | 9.21 | 0.30 | 0.30 |
| $TiO_2$ | - | 5.82 | 2.10 | 0.04 | 0.36 |
| CaO | 3.66 | 2.06 | 14.20 | 0.01 | 0.13 |
| MgO | - | 0.16 | - | 0.02 | 0.09 |
| $Na_2O$ | - | 11.32 | - | 0.03 | - |
| $K_2O$ | - | 0.38 | 1.60 | 0.14 | 0.49 |
| MnO | - | - | 0.09 | - | - |
| $SO_3$ | - | 0.32 | 1.60 | - | 1.00 |
| $Cr_2O_3$ | 2.06 | - | 0.03 | - | - |
| NiO | 3.06 | - | 0.01 | - | - |
| LOI at 1,000 °C | 7.32 | 7.96 | 5.37 | 0.56 | 7.66 |

A sintering temperature range of 1000–1200 °C was selected based on preliminary experiments and literature data, as this range is suitable for initiating crystallization in alumino-silicate-rich waste-derived glass-ceramic systems. This temperature window provides sufficient viscosity reduction for particle bonding while preventing excessive melting or deformation. A dwell time of 1 h was adopted to promote adequate phase transformation and crystal growth, essential for enhancing mechanical and physical properties. The raw materials were dry-ground in a ball mill for 30 min to achieve a particle size of $d_{100}$ = 100 μm under closed-loop conditions. The batch components were then homogenized using a laboratory mixer for 10 min. Each batch (75 ± 0.1 g) was prepared for the glass-ceramic test compositions. The binder (PVA) was dissolved in distilled water at 85 °C for 1 h and then mixed with the batch materials. The mixture was dried in an oven at 75 °C for 3 h. The dried powder was molded in a 15 cm³ oiled cylindrical steel mold and pressed for 2 min under 200 kg/cm² using a 30 T laboratory hydraulic press. Sintering of the green compacts was performed in an electrically heated muffle furnace between 1000 and 1200 °C for 2 h at a heating rate of 5 °C/min. Cooling occurred naturally within the furnace to room temperature. All sintering tests were repeated twice, producing four specimens for each experimental condition.

The apparent solid density ($\rho_a$) of the sintered specimens was determined according to ISO 18754:2020(E), Method A1 (liquid displacement under boiling conditions). The test piece was impregnated by maintaining it in a liquid under boiling conditions. For the calculation of the apparent solid density of the glass-ceramic [30, 31], an equation given below was applied:

$$\rho_a = \frac{m_1}{m_1 - m_2} \times \rho_1 \qquad (1)$$

where

$\rho_a$ is the apparent solid density, kg/m$^3$;

$m_1$ is the mass of the dry test specimen, kg;

$m_2$ is the apparent mass of the immersed test specimen, kg;

$\rho_1$ is the density of the immersion liquid at the temperature of the test, kg/m$^3$.

Water absorption was determined following EN 13755:2008 [32]. Dried specimens were weighed to a constant mass ($m_d$), immersed in water at atmospheric pressure for 48 h, then wiped with a damp cloth, and reweighed ($m_s$). Measurements were repeated every 24 h until a constant saturated mass was achieved. Water absorption ($A_b$) was calculated using Equation (2):

$$A_b = \frac{m_s - m_d}{m_d} \times 100 \qquad (2)$$

where
$m_d$ is the mass of the dry specimen, g;
$m_s$ is the mass of the saturated specimen,
g; $A_b$ is the water absorption at atmospheric pressure, %.

The compressive strength of the glass-ceramic specimens was evaluated using the Point Load Testing method in accordance with the International Society for Rock Mechanics (ISRM) standard [33]. The testing apparatus consisted of a point load frame with a pressure-measuring unit (Figure 1). The point load strength index ($Is_{50}$) was calculated using Equation (3):

$$Is_{50} = \frac{P}{D_e^2} \qquad (3)$$

where
*P* is the failure load (N).
*De* is the equivalent core diameter (cm).

For each composition, four specimens were tested, and the average $Is_{50}$ value was taken as the compressive strength of the material.

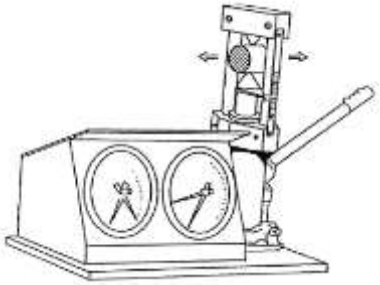

**Figure 1: The point load tester.**

### 3.1. Leaching of the Glass-Ceramics

The potential leachability of toxic substances from the produced glass-ceramics was evaluated following the Toxicity Characteristic Leaching Procedure (TCLP, Method 1311) [34]. Sintered glass-ceramic specimens were first ground to a particle size of <9.5 mm and then leached using an acetic acid solution adjusted to pH 2.88 ± 0.5, maintaining a liquid-to-solid ratio of 20:1 mL/g. The resulting leachates were filtered through 0.45 µm membrane filters and acidified with nitric acid to pH 2 prior to analysis. The concentrations of heavy metals in the leachates were determined using a PerkinElmer 900 H Atomic Absorption Spectrometer (AAS).

## 4. RESULTS AND DISCUSSION

### 4.1. Raw Materials

Silica and iron were the dominant components in the chromite tailings, while red mud was primarily composed of silica, iron, and aluminum oxides. Fly ash mainly contained silica and alumina (Table 1), consistent with the results of the XRD analyses. As shown in Figure 2a, the principal crystalline phases identified in the chromite waste were lizardite ($Mg_3(Si_2O_5)(OH)_4$), fayalite ($Fe_2SiO_4$), olivine ($(Mg,Fe)_2SiO_4$), and tridymite, a high-temperature polymorph of silica ($SiO_2$). The XRD pattern of red mud (Figure 2b) revealed quartz ($SiO_2$), ferrite spinel ($(Mg,Fe)(Fe,Al)_2O_4$), mullite ($Al_6Si_2O_{13}$), and hematite ($Fe_2O_3$) as the major phases. The F-class fly ash (Figure 2c) mainly contained quartz, mullite, and calcite. Among the additives, quartzite (Figure 3a) consisted of quartz, periclase (MgO), rutile ($TiO_2$), and muscovite ($KAl_2(AlSi_3O_{10})(F,OH)_2$), while kaolin (Figure 3b) contained kaolinite ($Al_2Si_2O_5(OH)_4$) and cristobalite ($SiO_2$), the latter being a high-temperature polymorph of silica formed above 1,400 °C.

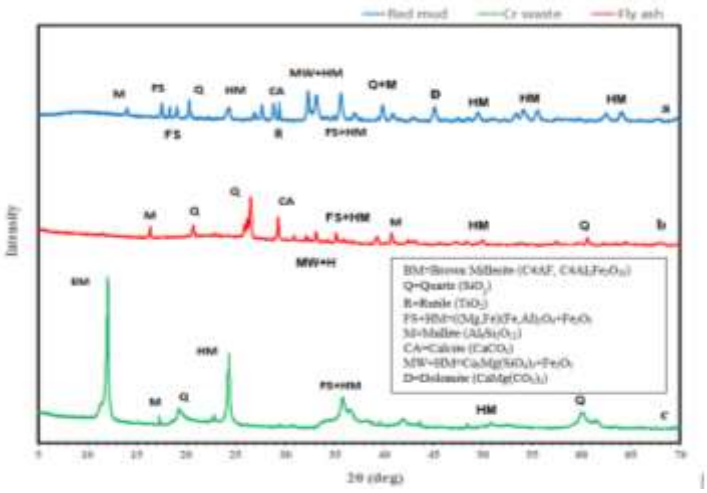


**Figure 2: Diffractograms of (a) red mud, (b) fly ash and (c) chromite waste (tailings).**

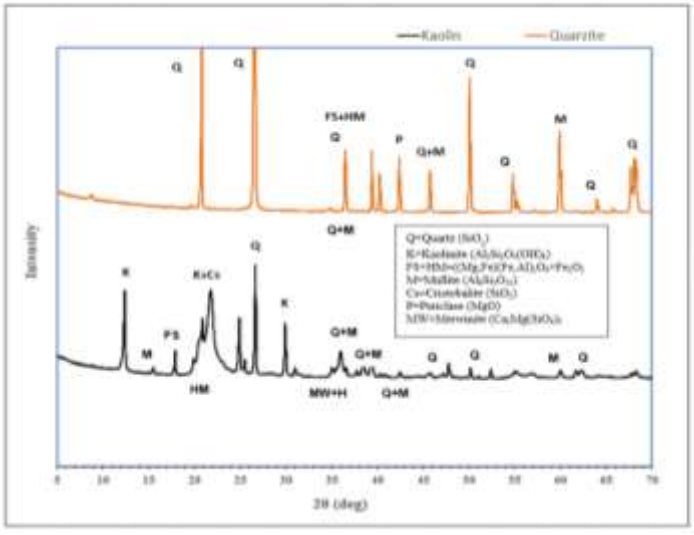


**Figure 3: Diffractograms of quartzite and kaolin.**

### 4.2. Properties of the Glass-Ceramics

Preliminary sintering tests were conducted to evaluate the effect of the mixing ratios (10–30 wt.%) of red mud, chromite tailings, and fly ash on glass-ceramic formation. Table 2 presents the three independent variables at three levels considered in the experimental design. After defining the waste mixture, the total mass of the green samples was adjusted to 100 wt. % by adding quartzite, while maintaining a constant 1:1 ratio of quartzite to kaolin. Sodium carbonate and PVA binder were added at 1.5 wt.% and 2 wt.%, respectively, of the total batch mass. Using the Taguchi approach where the number of experiments was $3^3 = 27$ although the experimental design of an orthogonal array required only nine experiments. This method uses a loss function to calculate the deviation between the experimental and desired values [28]. This loss function is converted into signal-to-noise (S/N) ratio.

Figure 4 shows the values of S/N ratio calculated based on S/N analysis. The effect of the production conditions can be easily determined from these graphs. As such, the effect of production conditions (from the highest to the lowest) was ordered as follows: red mud, fly ash, and chromite tailings. To obtain sintered glass with the highest point load index, the best material of the mixed/sintered sample should be prepared with a ratio of 1:2:3 (fly ash (Level 1), chromite tailings (Level 2), and red mud (Level 3)), which results in an obtain the sintered glass ceramics with a point load value of 12.21 MPa.

ANOVA results given in Table 4 indicates that the effects of production parameters on the preparation of the sintered glass were ordered as follows (from the highest to the lowest). The $R^2$ value was found to be 97.73% and the error ratio was calculated as 2.27%.

**Table 2: Production conditions for producing glass-ceramics and their levels (wt.%).**

| Parameters | Symbol | Level 1 | Level 2 | Level 3 |
|---|---|---|---|---|
| Red Mud | A | 10 | 20 | 30 |
| Chromite tailings | B | 10 | 20 | 30 |
| Fly ash | C | 10 | 20 | 30 |

The full factorial design with an orthogonal array of Taguchi L9 ($3^3$) for the experimental conditions needed for obtaining glass-ceramics is given in Table 3. It was aimed to obtain the product with higher point load index values. Therefore, the "larger is better" quality characteristic was used.

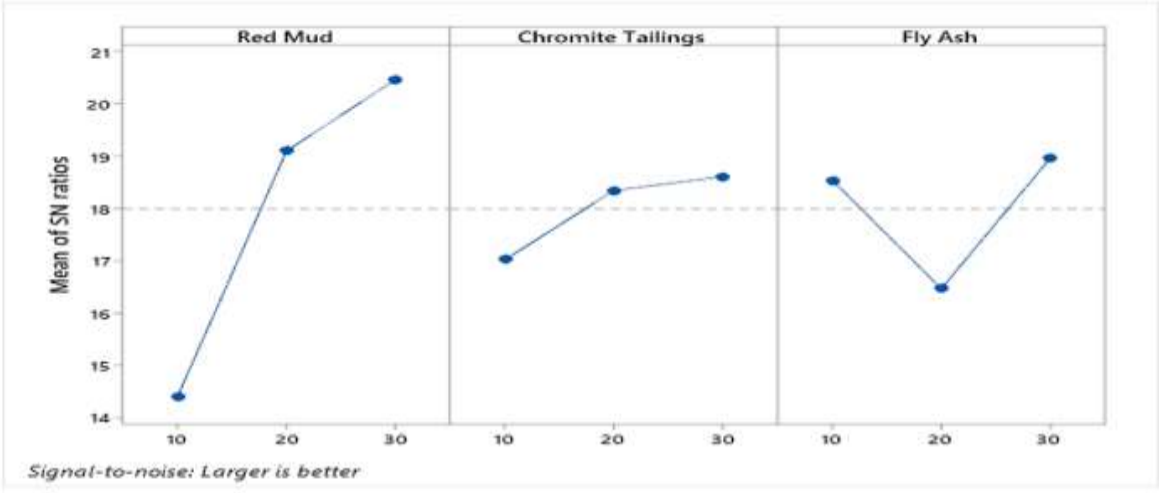


| Level | Red Mud | Chromite Tailings | Fly ash |
|---|---|---|---|
| 1 | 14,40 | 17,02 | 18,54 |
| 2 | 19,10 | 18,35 | 16,46 |
| 3 | 20,47 | 18,61 | 18,97 |
| Delta | 6,07 | 1,59 | 2,50 |
| Rank | 1 | 3 | 2 |

**Figure 4: S/N values of the experiments.**

For preliminary trials, green compacts were sintered at 1,200 °C for 2 h and annealed at 650 °C for 1 h [11, 28]. Temperature was identified as the key factor governing crystallization behavior and material properties. The resulting glass-ceramic samples exhibited reddish-black coloration due to the presence of iron and titanium oxides. Kaolin was kept constant in subsequent experiments as a dual source of $Al_2O_3$ and $SiO_2$, enhancing melt viscosity and structural stability at elevated temperatures. Further sintering tests (Table 5) were conducted to optimize the temperature conditions. The best-performing glass-ceramic produced from the 1:2:3 mixture displayed an apparent solid density of 2.05 g/cm³, average water absorption of 0.44%, and point load index of 12.21 MPa. XRD results (Figure 5) indicated that the dominant crystalline phases were quartz ($SiO_2$), rutile ($TiO_2$), and kaolinite, consistent with the mineral constituents of the raw materials. Microstructural examination using SEM (QUANTA FEG 650) revealed a vitreous, amorphous matrix with embedded crystalline phases and isolated pores (Figure 6). This microstructure contributed to the material's high density and compressive strength. For various pyro-metallurgical and refractory applications, particularly those based on spinel and mullite phases, understanding phase equilibria in the $Al_2O_3$–FeO–$Fe_2O_3$–$SiO_2$ system is crucial. Relevant studies in the literature have provided extensive experimental and thermodynamic modeling data for this system [28].

### 4.3. Leaching Behaviors of Cr After Thermal Processes

The concentrations of leached elements from the sintered glass-ceramic products are presented in Table 6. The results demonstrated that the heavy metal concentrations in the leachates were well below the regulatory limits specified by TCLP standards. Consequently, the glass-ceramic products derived from mining and metallurgical wastes can be safely utilized for household and construction applications, such as ceramic tiles [35, 36].

**Table 3: Full factorial design with an orthogonal array of Taguchi L9 ($3^3$).**

| Experiment no | Red Mud (wt.%) | Chromite tailings (wt.%) | Fly ash (wt.%) | Point load index (MPa) (mean values) | Visual appearance of prepared glass ceramics |
|---|---|---|---|---|---|
| 1 | 10 | 10 | 10 | 4.69 ± **0.07** |  |
| 2 | 10 | 20 | 20 | 4.69 ± **0.05** |  |
| 3 | 10 | 30 | 30 | 6.57 ± **0.07** |  |
| 4 | 20 | 10 | 20 | 7.05 ± **0.06** |  |
| 5 | 20 | 20 | 30 | 9.86 ± **0.09** |  |
| 6 | 20 | 30 | 10 | 10.56 ± **0.09** |  |
| 7 | 30 | 10 | 30 | 10.80 ± **0.1** |  |
| 8 | 30 | 20 | 10 | 12.21 ± **0.1** |  |
| 9 | 30 | 30 | 10 | 8.92 ± **0.07** |  |

**Table 4: ANOVA result of the experiments.**

| Source | DF | Adj SS | Adj MS | F-Value | P-Value |
|---|---|---|---|---|---|
| Red Mud | 2 | 45.329 | 22.6646 | 33.24 | 0.029 |
| Chromite Tailings | 2 | 3.404 | 1.7018 | 2.50 | 0.286 |
| Fly Ash | 2 | 9.940 | 4.9699 | 7.29 | 0.121 |
| Error | 2 | 1.364 | 0.6819 | | |
| Total | 8 | 60.036 | | | |

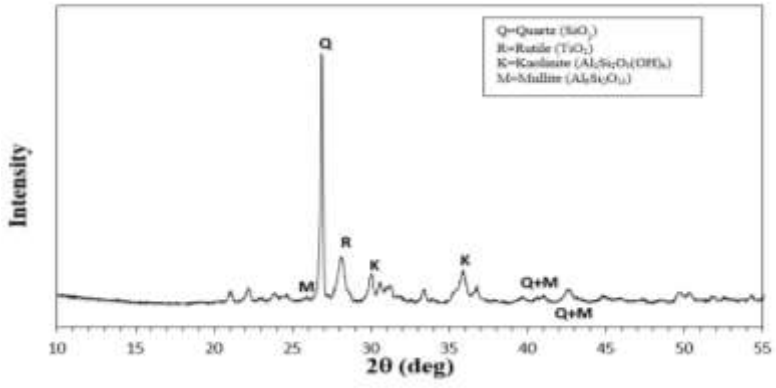


**Figure 5. Diffractograms of the glass-ceramic heat treated at 1,200 ˚C.**

**Table 5: Mix design of the prepared glass-ceramics.**

| | Reference | | | | |
|---|---|---|---|---|---|
| | **A1** | **B1** | **C1** | **D1** | **E1** |
| Chromite waste (g) | 20 | 20 | 20 | 20 | 20 |
| Red mud (g) | 30 | 30 | 30 | 30 | 30 |
| Fly Ash (Class F) (g) | 10 | 10 | 10 | 10 | 10 |
| Quartzite (g) | 20 | 20 | 20 | 20 | 20 |
| Kaolin (g) | 20 | 20 | 20 | 20 | 20 |
| Sodium carbonate (g) | 1.5 | 1.5 | 1.5 | 1.5 | 1.5 |
| Binding chemical (g) | 2 | 2 | 2 | 2 | 2 |
| Firing temperature (°C) | 1,000 | 1,100 | 1,200* | 1,200** | 1,200*** |
| Point load index (MPa) | 0.68 | 1.14 | 9.68 | 10.80 | 12.21 |
| Visual appearance of prepared glass ceramics |  |  |  |  |  |

* dwell time: 2 h
** dwell time: 30 min
*** no dwell time

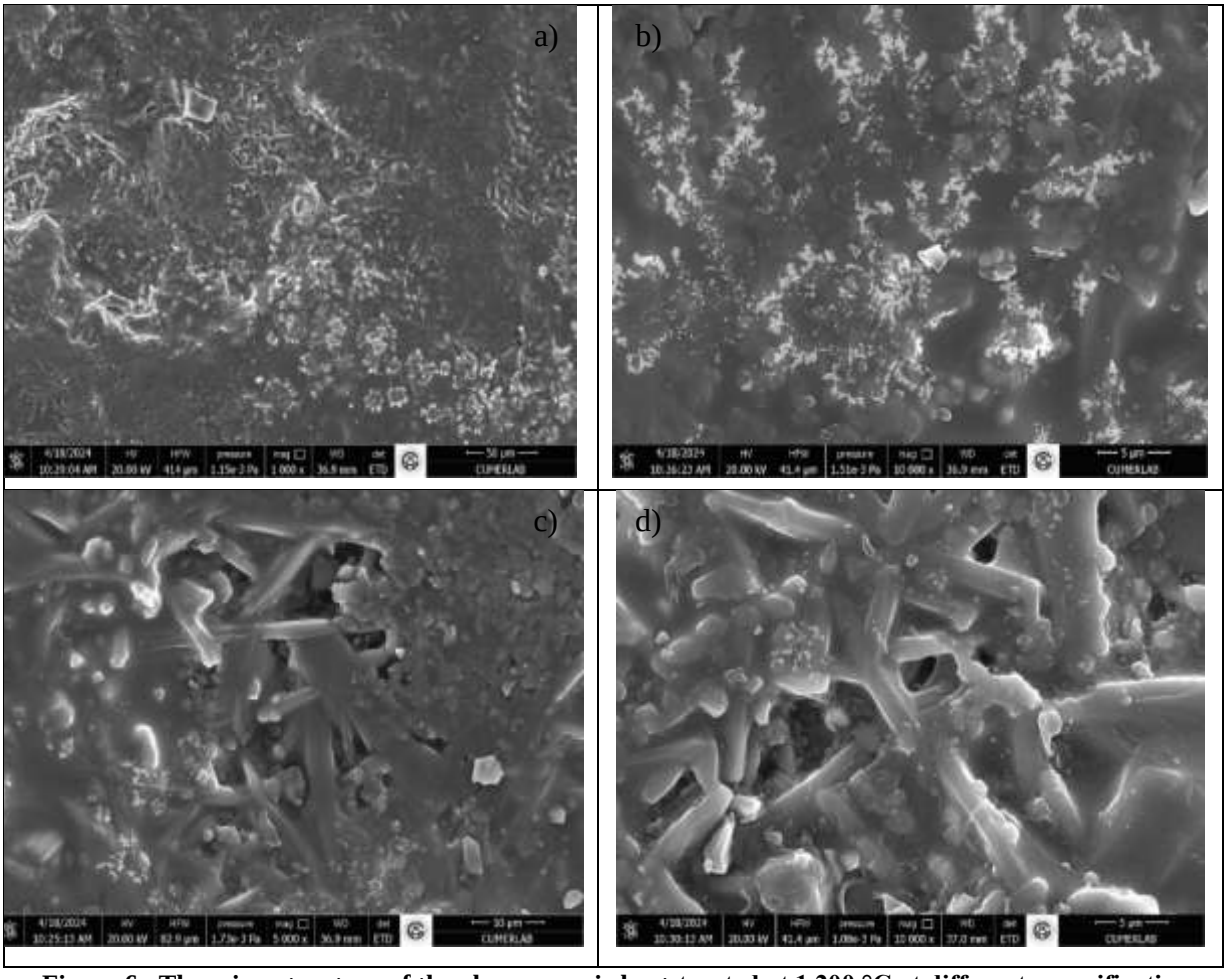


**Figure 6: The microstructure of the glass-ceramic heat-treated at 1,200 °C at different magnifications: (c) aggregates of needle-like mullite crystals growing from the surface toward the center of the glass particles, and (c) interlocked mullite crystals.**

**Table 6: Chemical analysis of the leachate from glass-ceramic product applying TCLP-Method 1311.**

| Element | The leachate (mg/L) |
|---|---|
| Mn | 0.14 |
| Al | nd (<1 mg/L) |
| Fe | 0.061 |
| Cr-total | nd (<0.1 mg/L) |
| Cu | 0.107 |
| Ti | nd (<1 mg/L) |
| Ni | nd (<0.1 mg/L) |
| Pb | nd (<0.1 mg/L) |
| Ca | 4.40 |

### 4.4. Potential Applications

In Türkiye, the production of environmentally friendly glass-ceramics is increasingly encouraged due to growing social and environmental awareness regarding energy consumption, waste accumulation, and depletion of natural resources. The valorization of industrial wastes such as red mud, chromite tailings, and fly ash offers a sustainable and low-cost pathway toward circular economy goals. Table 7 presents a comparative overview of the general properties of glass-ceramics for architectural applications, alongside similar materials reported in the literature [37-41].

In this study, only collection and grinding of the wastes to the required particle size were necessary, resulting in minimal production cost. However, the overall economic feasibility depends primarily on labor, waste transportation, energy consumption, operating costs, and governmental incentives. Therefore, further quantitative techno-economic and environmental assessments are recommended. The findings of this study suggest that waste-derived glass-ceramics provide an innovative, cost-effective, and environmentally sustainable waste management solution that promotes resource recovery and pollution mitigation.

**Table 7: Comparison of the physical and technological properties of building glass-ceramics along with the commercial products and the material produced in this study.**

| | **Glass-ceramic** [37] | | **Commercial Glass-ceramics (typical ranges)** [41]. | **Produced Material (This Study)** |
|---|---|---|---|---|
| | Conventional | Neoparis | | |
| Density, g/cm$^3$ | 2.4-3,6 | 2.7 | 2.4-2.8 | 2.05 |
| Compressive strength, (MPa) | n.a. | 12-56 | >1000 MPa | 12.21 (Point load index) |
| Water absorption, % | 1-5 | <1 | <0.5 | 0.44 |
| Porosity, % | - | - | <1–2% | n.a. |
| Hardness (Mohs) | - | - | 6-7 | n.a. |
| Thermal expansion (*10$^{-6}$ K$^{-1}$) | - | - | 5–9 | n.a. |
| Thermal shock resistance | - | - | High (better than glass, lower than ceramics) | n.a. |
| Acid/alkali resistance | - | - | Excellent | Excellent |
| Aesthetic properties | - | - | Glossy/matte, colorable, decorative designs | Glossy/matte, colorable, decorative designs |

## 5. CONCLUSION

This study demonstrated the feasibility of producing glass-ceramics from fly ash, chromite tailings, and red mud with an optimal 1:2:3 ratio. The resulting materials exhibited favorable physical and mechanical properties, including high density and strength, and showed no significant leaching of heavy metals. Although the study was limited by the lack of detailed microstructural and thermal analyses, limited replicates of mechanical tests, and absence of economic and environmental evaluations, it nonetheless provides a valuable foundation for future research. The results highlight the potential of integrating industrial waste valorization with sustainable material design, offering a promising approach for regions affected by extensive mining and metallurgical activities.

### Authors' Contributions

Oktay Bayat was primarily responsible for manuscript writing and data analysis, and contributed through critical review, editing, and overall supervision of the study. Mahmut Altiner and Muhammed Aboelgamel were responsible for specimen preparation, execution of experimental tests, and participation in data analysis.

## Declaration of competing interest

No known competing financial interests or personal relationships could have appeared to influence the study reported in this paper was declared by the authors.

## Data availability

Data will be made available on request.

## Acknowledgments

The authors wish to thank the support from Akmetal, Eti Alüminyum Corp., Sugözü thermal power plant, and Zafer Maden, Türkiye.

## References

[1] Wen Q., Liu B., Zhang J., Shen H., Deng J., and Zhang S., Glass-ceramics prepared from desulfurized electrolytic manganese residue and the nucleation promotion effect of calcium fluoride in glass phase transition, Ceramics International, 2024, 50(3), pp. 4563-4572.
[2] Tai Ceramic Society. 2025 cited 2025, Available from: http://www.thaiceramicsociety.com.
[3] Demir B.G., Özdoğan A.K., and Akbulut A., Türkiye krom potansiyeli, üretimi ve ihracatının genel bir değerlendirmesi, Uluborlu Mesleki Bilimler Dergisi, 2023, 6(1), pp. 92-101.
[4] Atasoy A., Reduction of ferric oxides in the red mud by the aluminıothermic process. in 6th International Advanced Technologies Symposium (IATS '11), 2011.
[5] Topal M., Topal E.I.A., Aslan S., and Kılıç M., Termik santral uçucu külü, cürufu ve arıtma çamurundan ağır metallerin liçlenebilirliği, Sakarya University Journal of Science, 2011, 15(2), pp. 97-104.
[6] Bayat O., Characterisation of Turkish fly ashes, Fuel, 1998, 77(9-10), pp. 1059-1066.
[7] Türker P., Erdoğan B., Katnaş F., and Yeğinobalı A., Türkiye'deki Uçucu Küllerin Siniflandirilmasi Ve Özellikleri, Ankara, Tçmb, 2009.
[8] Erkmen Z., Çataklı E., and Öveçoğlu L.M., Characterisation and crystallisation kinetics of glass ceramics developed from Erdemir blast furnace slags containing Cr2O3 and TiO2 nucleants, Advances in Applied Ceramics, 2009, 108(1), pp. 57-66.
[9] Li C., Zhang G., Zheng H., Zhang F., and Liu K., Characterization of glass-ceramics developed from zinc leaching residue by sintering method, Ceramics International, 2024, 50(5), pp. 8302-8317.
[10] Chen D., Wang Y., Yu Y., Ma E., and Zhou L., Microstructure and luminescence of transparent glass ceramic containing Er3+: BaF2 nano-crystals, Journal of Solid State Chemistry, 2006, 179(2), pp. 532-537.
[11] Huang Y., Chen Z., Liu Y., Lu J.-X., Bian Z., Yio M., Cheeseman C., Wang F., and Poon C.S., Recycling of waste glass and incinerated sewage sludge ash in glass-ceramics, Waste Management, 2024, 174, pp. 229-239.
[12] Xing J., Tang Q., Gan M., Ji Z., Fan X., Sun Z., Chen X., and Jing Q., Preparation of glass ceramic by low-temperature melting of municipal solid waste incineration fly ash and municipal sludge, Materials Letters, 2024, 359, pp. 135962.
[13] Li B., Chen C., Zhang Y., Yuan L., Deng H., and Qian W., Preparation of glass-ceramics from chromite-containing tailings solidified with Red Mud, Surfaces and Interfaces, 2021, 25, pp. 101210.
[14] Kritikaki A., Zaharaki D., and Komnitsas K., Valorization of industrial wastes for the production of glass–ceramics, Waste and biomass valorization, 2016, 7(4), pp. 885-898.
[15] Ismail N.Q.A., Sa'at N.K., Zaid M.H.M., Zainuddin N., and Mayzan M.Z.H., Effect of Na2CO3/Al2O3 ratio on the calcium fluoroaluminosilicate-based bioactive glass-ceramics derived from waste materials, Materials Chemistry and Physics, 2024, 312, pp. 128556.
[16] Luo Y., Bao S., and Zhang Y., Recycling of granite powder and waste marble produced from stone processing for the preparation of architectural glass–ceramic, Construction and Building Materials, 2022, 346, pp. 128408.
[17] Sang W., Yang X., Tian H., Wang J., Wang Y., and Li Z., Properties of SiO2-B2O3-Li2O-ZnO-Al2O3 glass-ceramic-coated diamond particles prepared by sol-gel method, Diamond and Related Materials, 2023, 139, pp. 110392.
[18] Jia Y., Xu B., Chi S., Xiang B., and Zhou Y., Research on the particle breakage of rockfill materials during triaxial tests, International Journal of Geomechanics, 2017, 17(10), pp. 04017085.
[19] Khater G., El-Kheshen A.A., and Farag M.M., High-performance glass-ceramics based on blast and arc furnace slag, Materials Chemistry and Physics, 2024, 311, pp. 128564.
[20] Prostakova V., Shishin D., Shevchenko M., and Jak E., Thermodynamic optimization of the Al2O3–FeO–Fe2O3–SiO2 oxide system, Calphad, 2019, 67, pp. 101680.
[21] Roy S. and Basu B., Hardness properties and microscopic investigation of crack–crystal interaction in SiO2–MgO–Al2O3–K2O–B2O3–F glass ceramic system, Journal of Materials Science: Materials in Medicine, 2010, 21(1), pp. 109-122.
[22] Zou W., Zhang W., Pi Y., Zhang Y., Chen Y., and Zhang L., Study on preparation of glass-ceramics from multiple solid waste and coupling mechanism of heavy metals, Ceramics International, 2022, 48(24), pp. 36166-36177.
[23] Yu Z., Liu Z., Ye F., and Xia L., Corrosion mechanism of magnesia-chrome and alumina-chrome refractories in E-scrap smelting, Ceramics International, 2022, 48(2), pp. 2693-2703.
[24] Agathopoulos S. and Tulyaganov D.U., Bioglasses and glass-ceramics in the Na2O–CaO–MgO–SiO2–P2O5–CaF2 system, Bioceramics and biocomposites: from research to clinical practice, 2019, pp. 123-148.
[25] Karasu B., Bereket O., Biryan E., and Sanoğlu D., The latest developments in glass science and technology, EL-Cezeri Journal of Science and Engineering, 2017, 4(2), pp. 209-233.
[26] Karasu B., Yanar A.O., Koçak A., and Kısacık Ö., Biyoaktif Camlar, EL-Cezeri Journal of Science and Engineering, 2017, 4(3), pp. 436-471.
[27] Özkan İ. and Dokumacı E., Recycling waste clay and rice husk ash in production of low density ceramics, EL-Cezeri Journal of Science and Engineering, 2021, 8(1), pp. 309-314.
[28] Yang J., Xiao B., and Boccaccini A.R., Preparation of low melting temperature glass–ceramics from municipal waste incineration fly ash, Fuel, 2009, 88(7), pp. 1275-1280.
[29] [DIN] D.I.f.N., General procedures for the X-ray fluorescence analysis (XRF) of oxidic raw materials, 2003.
[30] ISO, ISO 18754, Fine ceramics (advanced ceramics, advanced technical ceramics)—Determination of density and apparent porosity,, 2020.
[31] Erkmen Z., Ceramic Processing Techniques Laboratory Book, 2016.
[32] UNI E., 13755: 2008, Natural stone test methods-Determination of water absorption at atmospheric pressure, 2008.
[33] Franklin J., Suggested method for determining point load strength. in International Journal of Rock Mechanics and Mining Sciences & Geomechanics Abstracts, 1985, Elsevier.

[34] Akar G., Polat M., Galecki G., and Ipekoglu U., Leaching behavior of selected trace elements in coal fly ash samples from Yenikoy coal-fired power plants, Fuel processing technology, 2012, 104, pp. 50-56.
[35] Xu G., Zou J., and Li G., Stabilization of heavy metals in ceramsite made with sewage sludge, Journal of hazardous materials, 2008, 152(1), pp. 56-61.
[36] Li C., Zhang G., Zheng H., Zhang F., and Liu K., Study on glass-ceramic prepared by zinc leaching residue and solidification mechanism of heavy metals, Journal of Cleaner Production, 2023, 426, pp. 139021.
[37] Rincón J.M. and Romero M., Glass-ceramics as building materials, Materiales de construcción, 1996, 46(242-243), pp. 91-106.
[38] Khater G., Safwat E., Kang J., Yue Y., and Khater A., Some types of glass-ceramic materials and their applications, International Journal of Research, 2020, 7(4), pp. 1-16.
[39] Ponsot I.M., Pontikes Y., Baldi G., Chinnam R.K., Detsch R., Boccaccini A.R., and Bernardo E., Magnetic glass ceramics by sintering of borosilicate glass and inorganic waste, Materials, 2014, 7(8), pp. 5565-5580.
[40] Lu H.-x., He M., Liu Y., Guo J., Zhang L., Chen D., Wang H.-l., Xu H.-l., and Zhang R., Preparation and performance study of glass-ceramic glazes derived from blast furnace slag and fly ash, Journal of Ceramic Processing Research, 2011, 12(5), pp. 588-591.
[41] Ochen W., D'ujanga F.M., Oruru B., and Olupot P.W., Physical and mechanical properties of porcelain tiles made from raw materials in Uganda, Results in Materials, 2021, 11, pp. 100195.